Desalination and Water Treatment
www.deswater.com
doi: 10.1080/19443994.2015.1043498

57 (2016) 10111–10120
May

Taylor & Francis
Taylor & Francis Group

Effects of membrane transport properties and structure parameter on pressure-retarded osmosis performance

Yu Chang Kim[a,b,*], Sungyun Lee[a], Sang-Jin Park[a]

[a]*Department of Extreme Thermal Systems, Korea Institute of Machinery and Materials, Daejeon 305-343, Korea, Tel. +82 42 868 7397; email: kimyc@kimm.re.kr (Y.C. Kim)*
[b]*Environment & Energy Mechanical Engineering, Korea University of Science & Technology, Daejeon 305-350, Korea*

Received 15 January 2015; Accepted 16 April 2015

ABSTRACT

For salinity gradient power generation, a pressure-retarded osmosis (PRO) process uses a semipermeable membrane as a means of energy conversion. The performance of a PRO membrane is evaluated by the power density determined in a particular PRO condition. The membrane power density, which is the power generated per unit membrane surface area, can be calculated from the experimentally measured water flux and operating pressure difference. To fabricate a high-performance PRO membrane, both the transport properties and the structure parameter of the membrane should be balanced delicately. Water permeability (A) and salt permeability (B) are both transport properties of the active layer, while the structure parameter (S) is a distinct feature of the support layer. Thus, the PRO membrane should be designed to have three good parameters together. In addition, these A, B, and S parameters can be used in a PRO performance simulation to verify experimental results. In this study, the magnitude of effective osmotic pressures and reverse salt buildup factor is analyzed and a systematic investigation of the effect of the membrane transport properties and structure parameter on PRO performance is presented. The numerical simulation was performed for a number of actual and imaginary membranes. The imaginary membranes were both on A and B trade-off relationship and off the relationship. The A and S values affected the water flux value at a low pressure difference, while the B and S values influenced the water flux at high pressure. In addition, the effect of the mass transfer coefficient (k) in close connection with the experimental condition was examined. The k value was not an important variable in simulation, but it will play a significant role in a real-life process.

Keywords: Pressure-retarded osmosis; Membrane transport property; Structure parameter; Trade-off; Power density

1. Introduction

The pressure-retarded osmosis (PRO) process, which is a salinity gradient power generation technology, uses a semipermeable membrane as a means of energy conversion [1–8]. In PRO, independently introduced streams flow on both sides of the membrane. Unlike forward osmosis (FO), PRO requires a hydraulic pressure difference that is less

*Corresponding author.

Presented at GMVP Desalination Academic Workshop, Seoul, Korea, December 9, 2014

1944-3994/1944-3986 © 2015 Balaban Desalination Publications. All rights reserved.

than the osmotic pressure difference. Consequently, the direction of positive water permeation flux through a semipermeable membrane is against the hydraulic pressure gradient. Although the magnitude of water flux is determined by the osmotic pressure gradient, the hydraulic pressure difference has a greater influence than that of the osmotic pressure difference because of membrane performance limiting phenomena like concentration polarization (CP) and reverse salt diffusion (RSD) [9,10].

To date, no commercial membrane has demonstrated a membrane power density of 5 W/m^2 using fresh river water and seawater [11,12]. Of course, some research groups have recently reported that they have developed flat-sheet and hollow-fiber thin-film composite (TFC) PRO membranes with sufficiently high power density over 5 W/m^2 in research phase [13–19]. These PRO membranes are designed to have a thin, hydrophilic, and highly porous support layer for high water flux. The water flux in osmotically driven membrane processes, such as PRO and FO, is governed by membrane transport properties [20,21]. Accordingly, the water and salt permeability coefficients (A and B, respectively) of the membrane active layer and the structure parameter (S) of the membrane support layer are key characteristics determining transport performance of the membrane.

It is generally known that a PRO membrane with higher water permeability (A), lower salt permeability (B), and a lower structure parameter (S) is preferred. Among these three parameters, water permeability is closely linked to salt permeability because an increase in water permeability is accompanied by an increase in salt permeability and vice versa [10,22]. A suitable balance between A and B of the active layer also depends on the S parameter of the support layer. The low S value is essential to exploit a more permeable active layer, but at the same time causes the concomitant decline in selectivity [10].

As water and salt permeate across the membrane in the forward and reverse direction, respectively, the osmotic driving force is significantly reduced because of performance limiting phenomena such as internal and external concentration polarization (ICP and ECP) and RSD [10]. Due to the combined harmful effects of ICP, ECP, and RSD, the real water flux is much lower than the ideal value. These limiting effects in water flux and power generation were systematically analyzed in a previous study [10]. This analysis was mainly based on the trade-off between permeability and selectivity of the PRO membrane. However, according to recent PRO studies, all of the existing PRO membranes did not comply with this trade-off relationship because different fabrication methods and compositions of polymer material were used.

In this study, we present the individual effects of the A, B, and S parameters on PRO membrane performance. The characteristic parameters in literature are compared and PRO performance based on the values is numerically analyzed to determine the influence of the transport and structure parameters on water flux and power density. Impacts of the variation in these parameters on a straight line (J_W) and parabola (W) are analyzed. In addition, the effect of the mass transfer coefficient (k) in the boundary layer on water flux is investigated because it is included in ECP factor.

2. Basic theory

Water flux (J_W) through the membrane is defined as the flow rate permeated per unit membrane surface area. In PRO, J_W is actually calculated as a function of the osmotic pressure difference between draw and feed solutions ($\Delta\pi$), the hydraulic pressure difference (ΔP), and the water permeability coefficient of the membrane (A). The power density (W) of the membrane is also defined as the power generated per unit membrane surface area. W is obtained as a product of the water flux and the hydraulic pressure difference [23].

$$J_W = A(\Delta\pi - \Delta P) \tag{1}$$

$$W = J_W \times \Delta P = A(\Delta\pi - \Delta P)\Delta P \tag{2}$$

where J_W and W of the membrane are given in L m^{-2} h^{-1} and W m^{-2}, respectively. Theoretically, the power density (W) is a parabolic function of ΔP in which the maximum value (W_{max}) is at $\Delta P = \Delta\pi/2$. Optimal operating pressure is defined as the hydraulic pressure where W_m is reached. Thus, the maximum power density (W_{max}) is proportional to the water permeability coefficient and the square of the osmotic pressure difference ($W_{max} = A\Delta\pi^2/4$). If the target power density is 5 W m^{-2}, the water flux is calculated as 13.8 L m^{-2} h^{-1} at the optimal hydraulic pressure difference of 13 bar.

By the action of pressure applied, both solute and water tend to permeate the membrane. The water permeability coefficient (A) is determined by dividing the pure water permeate flux (J_W) by the applied hydraulic pressure (ΔP) [23]. The A value plays an important role since the membrane with a low A value will inevitably experience severe frictional resistance.

$$A = \frac{J_W}{\Delta P} \tag{3}$$

The salt (NaCl) rejection (R) is determined using salt-containing feed solution. Based on conductivity measurements, the R value is calculated from the feed (C_f) and permeate (C_p) salt concentrations ($R = (C_f - C_p)/C_f$), and then the salt (NaCl) permeability coefficient (B) is determined from [23]:

$$B = \left(\frac{1-R}{R}\right) J_W = \left(\frac{1-R}{R}\right) A(\Delta P - \Delta\pi) = \left(\frac{1-R}{R}\right) J_W \exp\left(-\frac{J_W}{k}\right) \tag{4}$$

where k is the mass transfer coefficient for the cross-flow channel of the membrane cell.

The structure parameter (S) of the support layer is defined as [11,12]:

$$S = \frac{t_S \tau}{\varepsilon} \tag{5}$$

where t_S is the support layer thickness, τ is the tortuosity, and ε is the porosity. The S value is the characteristic distance the salt needs to diffuse through and has unit of length. Since a large S value leads to severe ICP, relatively thin membranes with low tortuosity and high porosity are preferred [11–13]. The low S value minimizes the effective thickness of the ICP unstirred diffusive boundary layer, thereby allowing for higher water flux and power density.

The high J_W and W in PRO is achieved by ideal conditions such as large water permeability (A), small salt permeability (B), and small structure parameter (S) values. Here, the A and B values are related to the active layer, while the S value is an attribute of the support layer. However, because these parameters are intertwined, it is difficult to improve them individually. Accordingly, to meet the target power density of 5 W/m^2, the PRO membrane will need to possess a small structure parameter if possible, together with balanced active layer transport properties [10,13]. However, their effects on various mechanisms are extremely intricate, and it is difficult to optimize the three parameters simultaneously.

Water and salt ions are commonly understood to permeate through the nonporous active layer according to the solution-diffusion mechanism [24]. Usually, polymer materials that are more permeable to water are often less selective, and vice versa. This permeability–selectivity trade-off relation governs TFC membranes in real situations [22]. The polyamide (PA) active layer is subjected to a chlorine-alkaline post-treatment to modulate the water and salt permeabilities [10]. This chlorine-alkaline treatment enhances the water permeability of the PA active layer at the expense of selectivity of salt. Accordingly, the A and B values of the PRO membrane conform to a correlation equation [10,25].

$$B = \lambda A^{\beta} \tag{6}$$

where $\lambda = 0.0133$ and $\beta = 3$. The empirically derived equation indicates that B value is proportional to A^3. In other words, salt permeability increases faster than the increase in water permeability. Thus, a delicate balance between A and B is strategically important to achieve a high water flux, since these two properties cannot be controlled independently of each other.

The water flux during the PRO process is governed by several performance limiting phenomena such as ECP, ICP, and RSD. Accordingly, the theoretical water flux equation is represented as follows [13]:

$$J_W = A\left[\frac{\pi_{D,b} \exp\left(-\frac{J_W}{k}\right) - \pi_{F,b} \exp\left(\frac{J_W S}{D}\right)}{1 + \frac{B}{J_W}\left[\exp\left(\frac{J_W S}{D}\right) - \exp\left(-\frac{J_W}{k}\right)\right]} - \Delta P\right] \tag{7}$$

where $\exp(-J_W/k)$, $\exp(J_W S/D)$, and $1 + (B/J_W)[\exp(J_W S/D) - \exp(-J_W/k)]$ are ECP, ICP, and the reverse salt buildup factor, respectively, and D included in these factors is the diffusion coefficient of the feed solute. The osmotic pressure of the draw solution is reduced by the ECP factor and that of the feed solution is magnified by the ICP factor. Thus, the osmotic pressure difference across the membrane becomes smaller. The water flux declines dramatically with an increase in feed concentration because the ICP factor is over 1. Most importantly, the detrimental effect of ICP is intensified by the RSD, meaning salt permeation from the more concentrated draw solution into the feed solution [10]. The permeated salt accumulates in the porous support layer and further dramatically reduces the osmotic driving force. Especially in high pressure, this adverse effect of RSD coupled with ICP significantly countervails the benefit of high water permeability.

The water permeability coefficient (A), salt permeability coefficient (B), and salt rejection (R) of the PRO membrane are experimentally determined in RO condition ($\Delta P > \Delta\pi$) [19]. The A value is measured using deionized (DI) water and the B and R values are obtained for the NaCl solution of a particular

concentration. The structure parameter (S) of the PRO membrane is calculated from the FO ($\Delta p = 0$) or PRO ($\Delta P < \Delta\pi$) experiments [19]. These membrane transport properties and structure parameter obtained through the RO and FO (or PRO) experiments enable us to predict accurately the membrane water flux and resulting power density in PRO. To determine the theoretical water flux (J_W), the above PRO water flux model was solved numerically using the membrane transport properties, the osmotic pressures of draw and feed solution (π_D and π_F, respectively), and the hydraulic pressure difference (ΔP). Ideally, the water flux decreases linearly, and the power density shows a convex curve with a peak value. However, because the modeled water flux depends on the membrane transport properties, it is not exactly linear. Since the salt rejection of the membrane is not perfect, maximum power density occurs at $\Delta P < \Delta\pi/2$. As the salt rejection of the membrane decreases, the theoretical flux reversal pressure becomes lower than the ideal flux reversal pressure.

3. Results and discussion

3.1. Effective osmotic pressures and reverse salt buildup factor

As indicated previously, the theoretical PRO water flux equation contains several terms related to ECP, ICP, and RSD. Osmotic driving force is reduced due to the detrimental effects of the three factors. The effective osmotic pressure of the draw solution is the bulk osmotic pressure of the draw solution multiplied by the ECP factor, $\pi_{D,b} \exp(-J_W/k)$. Similarly, the effective osmotic pressure of the feed solution is the bulk osmotic pressure of the feed solution multiplied

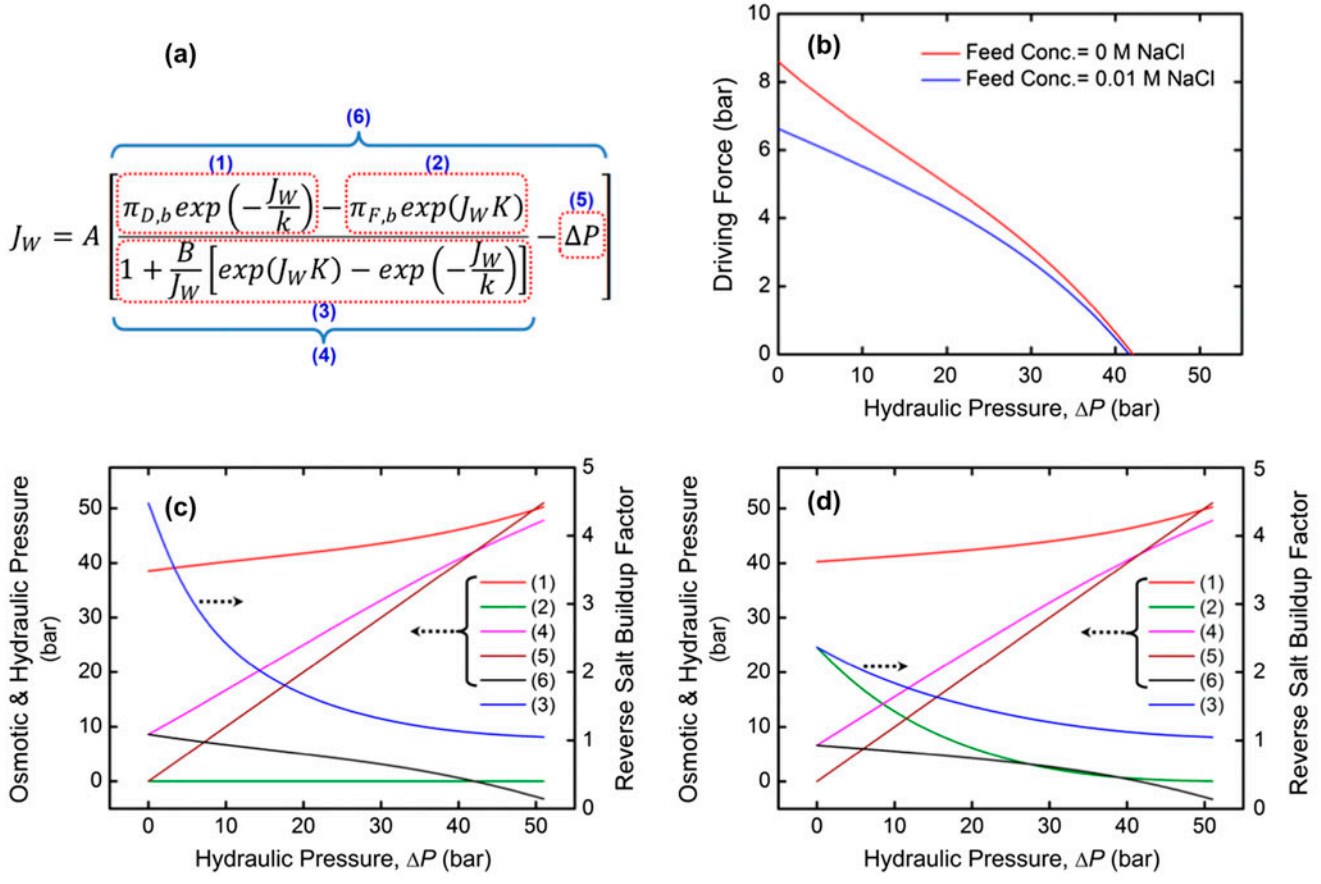

Fig. 1. The magnitude of all terms in driving force of PRO water flux equation. (a) PRO water flux equation: (1) draw osmotic pressure with ECP, (2) feed osmotic pressure with ICP, (3) reverse salt buildup factor, (4) effective osmotic pressure difference, (5) hydraulic pressure difference, and (6) effective driving force, (b) comparison of effective driving forces for different feed concentrations, (c) osmotic and hydraulic pressures for DI feed water, (d) osmotic and hydraulic pressure for 0.01 M NaCl feed solution. 1 M NaCl draw solution is used in all calculations.

Table 1
Membrane transport properties and structure parameters

Sample no.	A (L m^{-2} h^{-1} bar^{-1})	B (L m^{-2} h^{-1})	B/A (bar)	S (μm)	Membrane type	Manufacturer	Ref.
1	0.36	0.32	0.90	595	CTA (FS)	HTI[a]	[13]
2	0.37	0.28	0.74	590	CTA (FS)	HTI	[26]
3	0.66	0.42	0.64	694	CTA (FS)	HTI	[19]
4	2.49	0.39	0.16	564	TFC (FS)	HTI	[17]
5[b]	1.63	0.11	0.07	349	TFC (FS)	Yale U.	[13]
6	1.20	0.20	0.17	600	TFC (FS)	NUS[c]	[18]
7	3.12	0.55	0.18	1,022	TFC (FS)	Toray[d]	[19]
8	3.32	0.14	0.04	460	TFC (HF)	NTU[e]	[14]
9	1.90	0.48	0.25	776	TFC (HF)	NUS	[15]
10	3.30	0.31	0.09	450	TFC (HF)	NUS	[16]

[a]HTI: Hydration Technology Innovations.
[b]Among three different membrane formulations, the TFC membrane used in this study is a low permeability membrane.
[c]NUS: National University of Singapore.
[d]Woongjin Chemical Co. as was.
[e]NTU: Nanyang Technological University.

by the ICP factor, $\pi_{F,b}$ exp ($J_W S/D$). Accordingly, the effective osmotic driving force is the difference between $\pi_{D,b}$ exp ($-J_W/k$) and $\pi_{F,b}$ exp ($J_W S/D$).

In addition, the dramatic increase in RSD accumulates salt within the porous support layer and reduces the effective osmotic driving force. This RSD is an important phenomenon in osmotically driven membranes like PRO and FO membranes. That is, the osmotic pressure difference is reduced by the RSD factor in the denominator, $1 + B/J_W$[exp ($J_W K$) – exp ($-J_W/k$)]. Since the water flux (J_W) value is included in these three factors, and since J_W decreases with increasing pressure, these three terms are functions of the hydraulic pressure difference.

Fig. 1 compares the magnitude of all terms in the PRO water flux equation. For this calculation, two solutions (DI water and 0.01 M NaCl solution) were used as feed solutions to investigate the effect of feed solution concentration. One molar NaCl draw solution was an opponent for two feed solutions. Eq. (7) was segregated to several terms as follows: (1) draw osmotic pressure with the ECP, (2) feed osmotic pressure with the ICP, (3) reverse salt buildup factor, (4) effective osmotic pressure difference, (5) hydraulic pressure difference, and (6) PRO effective driving force. Here, all terms except the reverse salt buildup factor have a unit of pressure (bar). The ECP and osmotic driving force terms "(1) and (4)" increased with an increasing hydraulic pressure difference because the degree of dilution was decreased due to the reduction of water permeation. On the contrary, the ICP and RSD terms "(2) and (3)" decreased with an increasing hydraulic pressure difference because the degree of

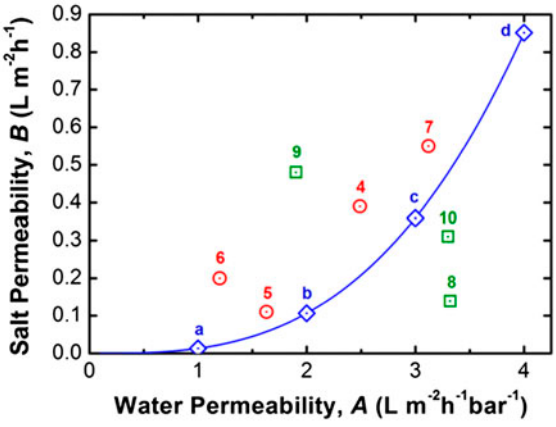

Fig. 2. Water and salt permeability coefficients of TFC PRO membranes. Red circle and green square dots indicate flat-sheet and hollow-fiber membranes reported in recent publications, respectively. Solid blue line and diamond dots represent the A and B trade-off relationship (B = 0.0133 A^3). Data for each dot were used for J_W and W calculation.

concentration decreased due to the reduction of water permeation.

For the DI water feed solution, the ICP term "(2)" was negligible but for the 0.01 M NaCl feed solution, it was considerable as shown in Fig. 1(c) and (d), respectively. The RSD term "(3)" decreased exponentially with an increasing hydraulic pressure difference. The magnitude of the RSD factor at the use of the DI water feed solution was higher than that at the use of the 0.01 M NaCl feed solution because of the extent of reverse diffusion resulting from concentration

difference. Consequently, as the feed concentration increased, the ICP effect exacerbated and the ICP term resulted in the reduced effective osmotic pressure difference. The ICP effect reduced the water flux significantly at low pressures, but gradually diminished because water flux became smaller at high pressures.

3.2. Modeled PRO performance (J_W and W) of TFC PRO membranes

Water and salt permeabilities are intrinsic material properties and are independent of measurement conditions. Most of the TFC membranes show a trade-off relationship between selectivity and permeability. Membranes with high selectivity will have relatively low permeability, and vice versa. Table 1 presents the membrane characteristic properties of some PRO and FO membranes reported in literature [13–19,26]. Some membranes (No. 1–3) are cellulose triacetate (CTA) based FO membranes, while the other membranes (No. 4–10) are TFC PRO membranes. For membrane type, numbers "1–7" are flat-sheet membranes and numbers "8–10" are hollow-fiber membranes. CTA membranes showed low A and high B values. Thus, the B/A values of CTA membranes were relatively high. The effective osmotic pressure due to RSD can be roughly estimated by the B/A value. Since TFC membranes had a higher A value than CTA membranes, the B/A value was relatively small. Membrane "No. 9" had the highest B/A value, while membrane "No. 8" had the lowest B/A value. Membranes "No. 4, 6, and 7" had similar B/A values.

Fig. 2 is a plot of water and salt permeabilities of TFC PRO membranes in Table 1. The red circle and green square dots indicate flat-sheet (No. 4–7) and hollow-fiber (No. 8–10) membranes. Blue diamond dots represent the specific value (A = 1, 2, 3, and 4) in correlation to the equation. Of course, CTA

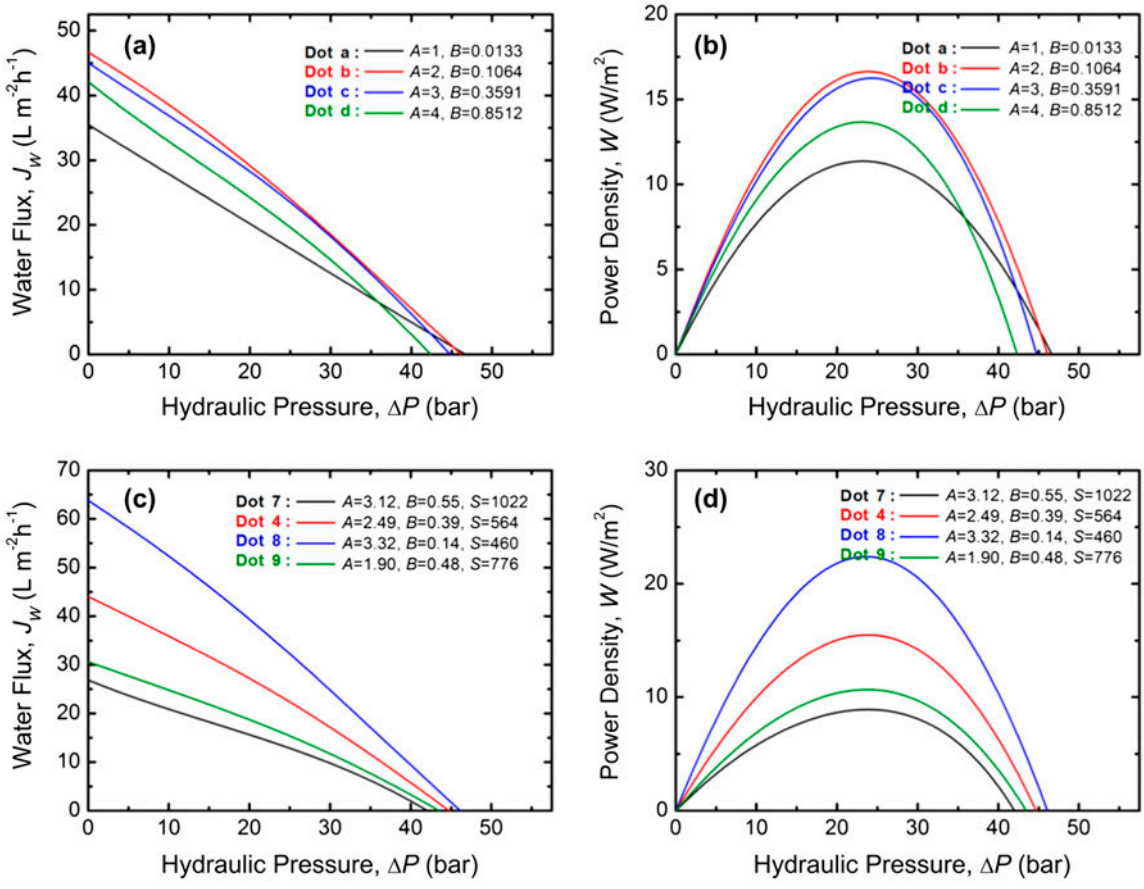

Fig. 3. Modeled water flux (J_W) and the respective power density (W) for each dot in Fig. 2. Here, J_W and W for 1 M NaCl draw solution (π = 46.75 bar) and DI water feed solution were calculated. (a) and (b) J_W and W for PRO membranes with A and B trade-off correlation, respectively. The structure parameter and mass transfer coefficient used in the calculations are S = 600 μm and k = 138.6 L m^{-2} h^{-1}, respectively. (c) and (d) J_W and W for PRO membranes reported in recent publications, respectively. ECP mass transfer coefficient is k = 138.6 L m^{-2} h^{-1}.

membranes do not appear in the figure because they do not follow the A and B trade-off relationship. The trade-off correlation equation used was based on a fit to the experimentally determined permeability values from hand-cast membranes developed in a laboratory. Thus, most of the recent membranes deviated remarkably from the trade-off equation. Most importantly, two membranes (No. 8 and 9) were very far from the curved line. This was because fabrication methods, materials, types, and the structure parameter (S) of membranes, and experimental conditions differed from laboratory to laboratory. Slight variations in experimental conditions can have a profound influence on water flux and salt rejection.

For dots "a, b, c, and d" on the trade-off correlation equation, the performance simulation results are presented in Fig. 3(a) and (b). Here, $S = 600$ μm and $k = 138.6$ L m^{-2} h^{-1} were used for the modeling where they were not variables. The B/A values for dots "a, b, c, and d" were as follows: 0.0133, 0.0532, 0.1197, and 0.2128. The B/A value of dot "d" was larger than that of dot "a" but the performance of dot "d" was higher than that of dot "a". When the A value increased from 1 to 2, the corresponding water flux increased. But when the A value increased over 2, the corresponding flux decreased because the B value increased much faster. As the B value increased, the flux reversal pressure became smaller. Accordingly, the relationship between J_W and ΔP became nonlinear. Thus, the optimal operating pressure difference for the maximum power density was less than the $\Delta\pi/2$ value. A high salt permeability negatively impacted PRO performance. It accelerated the water flux decline with increasing hydraulic pressure. A major cause of the different decreasing trends in water flux resulted from the different salt permeabilities.

Fig. 3(c) and (d) exhibit the modeled results for actual membranes off the trade-off relationship. The mass transfer coefficient of 138.6 L m^{-2} h^{-1} was used for the modeling. The B/A values for dots "4, 7, 8, and 9" were as follows: 0.16, 0.18, 0.04, and 0.25. For membranes with a similar structure parameter, the water flux decreased with an increasing B/A value. Since dot "7" had a lower B/A value than dot "9" but a higher S value, dot "7" showed lower water flux than dot "9". Dot "4" and dot "7" had similar B/A values but two membranes exhibited considerable difference due to the possession of a different S value. A high salt permeability significantly reduced the power density at high hydraulic pressures because of its adverse effect on the effective osmotic driving force. In a large-scale membrane module, the permeated salts will increase the feed solution salinity, and dramatically reduce the power density of the module.

3.3. *Effects of* A, B, *and* S *parameter variations on PRO performance*

In the previous section, the A, B, and S values of actual fabricated membranes were used in a performance simulation. As such, individual effects were not able to be identified. In this section, we investigated the individual effects of the water and salt permeability coefficients (A and B) and structure parameter (S) on the water flux (J_W) and the respective power density (W). Membrane "No. 7" with relatively high B and S values in Table 1 was selected to investigate the individual effect of each parameter. In Fig. 4, red circle "a" shows the transport properties of the PRO membrane determined in our previous study [19]. Red circles "b–e" indicate the predetermined transport properties. Half and double of original values are displayed in the figure. Of course, the S value varies by half or double just like A and B values. Here, the water and salt permeability coefficients (A and B) trade-off relationship was not considered for individual effects.

For all J_W and W simulations, 1 M NaCl draw solution and DI water feed solution were used as high and low salinity solutions, respectively. $A = 3.12$ L m^{-2} h^{-1} bar^{-1}, $B = 0.55$ L m^{-2} h^{-1}, $S = 1{,}022$ μm, and $k = 138.6$ L m^{-2} h^{-1} were used for the PRO performance simulation, when they were not variables. When the A value changed, the theoretical flux reversal pressure remained the same, whereas when B or S values changed, the theoretical flux reversal pressure also changed. Hence, for variation of water permeability, optimal pressure for the maximum power density remained almost the same, but for the variation of salt permeability, the optimal pressure changed. This

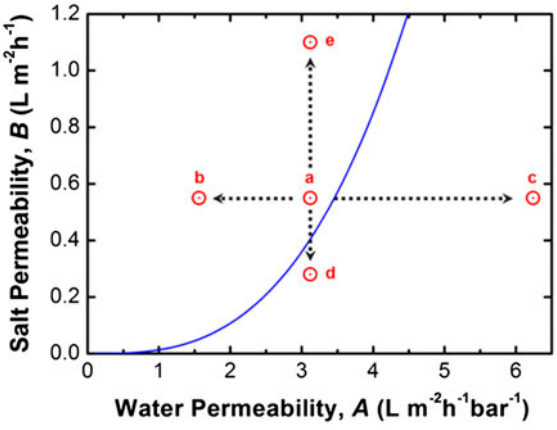

Fig. 4. Water and salt permeability coefficients of TFC PRO membranes. Red circle dot "a" indicates the A and B values of the PRO membrane obtained in our previous study. Red circle dots "b–e" indicate data for imaginary membranes. Blue line represents the A and B trade-off relationship ($B = 0.0133\ A^3$).

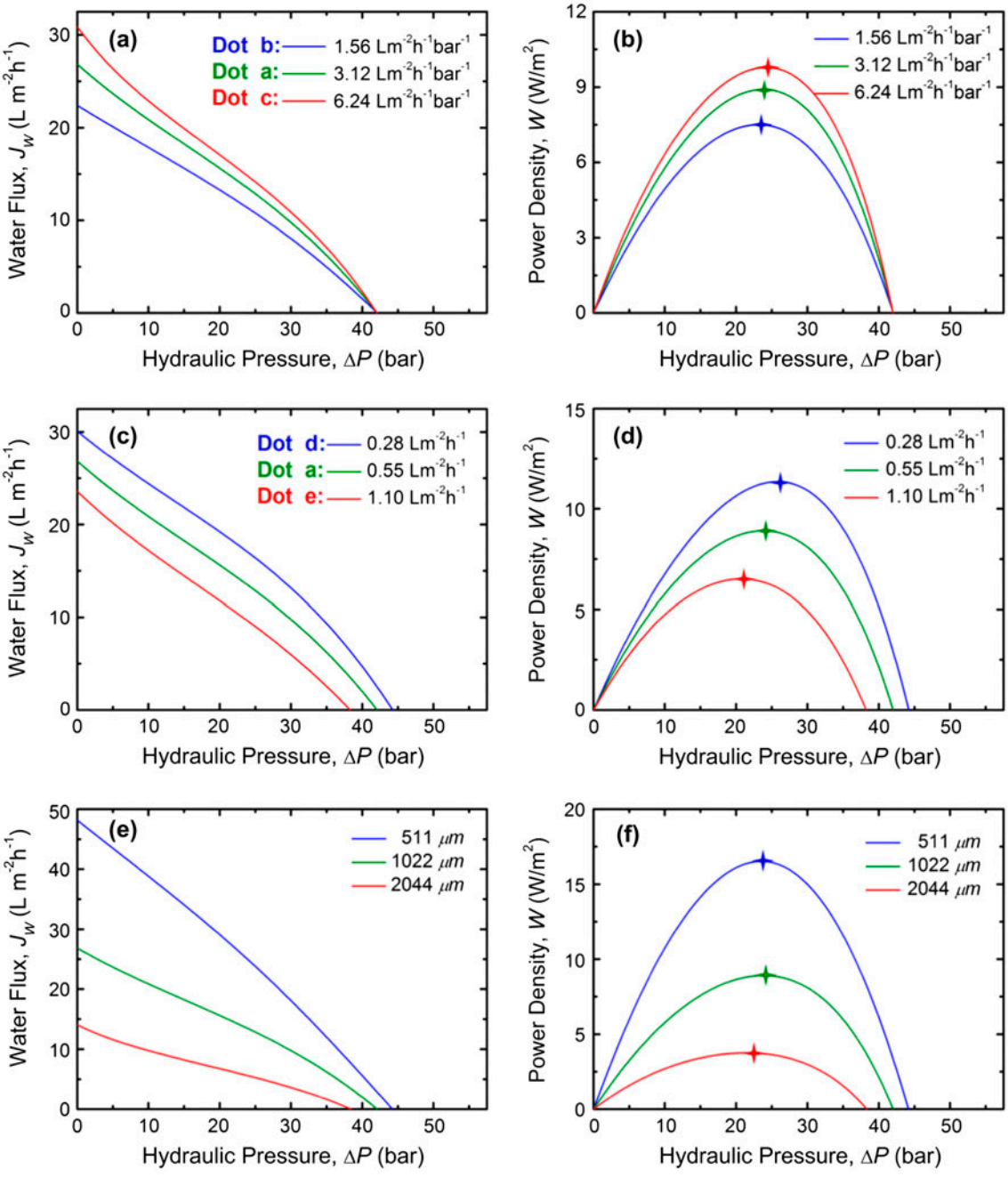

Fig. 5. Variation effect of water and salt permeability coefficients (A and B, respectively) and structure parameter (S) on modeled water flux (J_W) and the respective power density (W). As reference values, J_W and W for 1 M NaCl draw solution (π = 46.75 bar) and DI water feed solution were calculated using A = 3.12 L m^{-2} h^{-1} bar^{-1}, B = 0.55 L m^{-2} h^{-1}, S =1,022 μm, and k = 138.6 L m^{-2} h^{-1} (green lines in all graphs). To investigate individual effects, we changed one predetermined parameter to half (blue line) or double (red line) the reference value and fixed the others. (a and b) A is a variable (c and d) B is a variable, and (e and f) S is a variable.

was because the salt permeability directly impacted the effective osmotic pressure difference.

A higher value A resulted in better membrane power density, whereas lower B or S values resulted in better performance. From Fig. 5, each transport property seemed to have its own role. The water permeability coefficient (A) affected the y-intercept on the y-axis of the water flux graph (Fig. 5(a)). Since the flux reversal pressure was a pivot, the variation range was higher at low pressure. The salt permeability

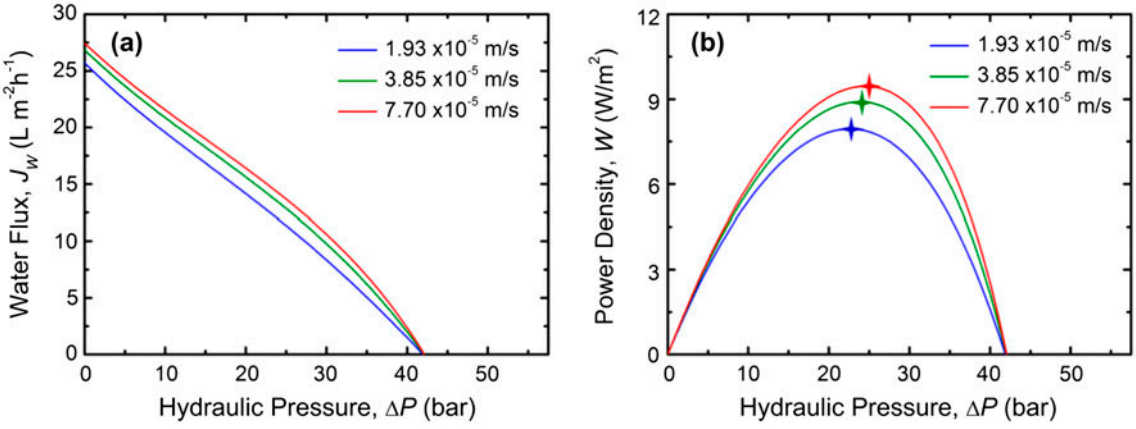

Fig. 6. Variation effect of mass transfer coefficients (k) on modeled water flux (J_W) and the respective power density (W) as a function of applied hydraulic pressure difference (ΔP). (a and b) J_W and W for 1 M NaCl draw solution (π = 46.75 bar) and DI water feed solution were calculated using A = 3.12 L m^{-2} h^{-1} bar^{-1}, B = 0.55 L m^{-2} h^{-1}, and S = 1,022 μm, respectively.

coefficient (B) gave rise to parallel displacement in the y-axis direction of the water flux graph without a pivot (Fig. 5(c)). That is, a smaller salt permeability coefficient (B) moved the flux reversal pressure near the calculated osmotic pressure difference; and hence, a smaller B was essential to enhance the peak power density.

The membrane with half of the original B value had higher power density than that with double the original A value. An imaginary membrane designated by "d" had the power density of 11.39 W/m^2 and another imaginary membrane marked "c" had 9.84 W/m^2. The imaginary membranes, in order of decreasing power densities, were "d, c, a, b, and e". Interestingly, the structure parameter (S) cut in half raised markedly the y-intercept in the y-axis of the water flux graph and maintained the effect of osmotic pressure as a driving force over the whole pressure range (Fig. 5(e)). Like this result, the performance of osmotically driven membranes such as PRO membranes was greatly influenced by the structure parameter (S). Although the active layer transport properties of two membranes were equal, the different structural factors of porous support layers resulted in a considerable difference in PRO performance.

3.4. Effects of the mass transfer coefficient (k) variation on PRO performance

Similar to the effect of water permeability, the flux reversal pressure was nearly unaffected despite the varying mass transfer coefficient (k), as shown in Fig. 6. Of course, a higher k value resulted in better membrane power density, but the influence of k on J_W was less than that of A, B, and S. This was because the exp ($-J_W/k$) term involving k ranged from 0 to 1. The mass transfer coefficient (k) affected the y-intercept on the y-axis of the water flux graph, but the effects of the k value were not noticeable. Because the flux reversal pressure was a pivot, the performance variation range was higher at low pressure.

The mass transfer coefficient depends on experimental conditions such as superficial velocity in flow channel, voidage of spacer used, and temperature, etc. [27–30]. Thus, the mass transfer coefficient can be enhanced by improving the mixing at the membrane interface through the increased crossflow velocity, or the use of spacers [29,30]. However, the trade-off for a higher mass transfer rate is an increased pressure drop along the channel, while the energy consumption of the pump is increased with an increasing superficial velocity. Nevertheless, the enhancement of the mass transfer rate will be important for a module with a large membrane area.

4. Conclusions

The transport properties and structural factor of a membrane complexly influenced PRO performance. Both salt permeability and the structural factor directly impacted the osmotic pressure difference because a RSD phenomenon was exhibited in the PRO membrane. The effective feed osmotic pressure and reverse salt buildup factor was considerably high and reduced the effective osmotic pressure difference. Hence, the slope of hydraulic pressure difference was steeper than that of effective osmotic pressure difference. Generally, the A and S values affected the water flux value at a low pressure difference while the B and S values influenced the water flux at a high pres-

sure. That is, in the J_W graph, the A and S values determined the y-intercept, while the B and S values determined the x-intercept. The k value was not an important variable in simulation, but will play a significant role in a real process.

Acknowledgements

This research was supported by a grant (code 13IFIP-B065893-01) from the Industrial Facilities & Infrastructure Research Program funded by Ministry of Land, Infrastructure and Transport of Korean government.

References

[1] B.E. Logan, M. Elimelech, Membrane-based processes for sustainable power generation using water, Nature 488 (2012) 313–319.
[2] F. Helfer, C. Lemckert, Y.G. Anissimov, Osmotic power with pressure retarded osmosis: Theory, performance and trends—A review, J. Membr. Sci. 453 (2014) 337–358.
[3] A. Achilli, A.E. Childress, Pressure retarded osmosis: From the vision of Sidney Loeb to the first prototype installation—Review, Desalination 261 (2010) 205–211.
[4] S. Loeb, Production of energy from concentrated brines by pressure-retarded osmosis: I. Preliminary technical and economic correlations, J. Membr. Sci. 1 (1976) 49–63.
[5] S. Loeb, F. Van Hessen, D. Shahaf, Production of energy from concentrated brines by pressure-retarded osmosis: II. Experimental results and projected energy costs, J. Membr. Sci. 1 (1976) 249–269.
[6] S. Loeb, Energy production at the Dead Sea by pressure-retarded osmosis: challenge or chimera? Desalination 120 (1998) 247–262.
[7] S. Loeb, One hundred and thirty benign and renewable megawatts from Great Salt Lake? The possibilities of hydroelectric power by pressure-retarded osmosis, Desalination 141 (2001) 85–91.
[8] S. Loeb, Large-scale power production by pressure-retarded osmosis, using river water and sea water passing through spiral modules, Desalination 143 (2002) 115–122.
[9] S. Loeb, A two-coefficient water transport equation for pressure-retarded osmosis, J. Membr. Sci. 4 (1979) 351–362.
[10] N.Y. Yip, M. Elimelech, Performance limiting effects in power generation from salinity gradients by pressure retarded osmosis, Environ. Sci. Technol. 45 (2011) 10273–10282.
[11] K. Gerstandt, K.V. Peinemann, S.E. Skilhagen, T. Thorsen, T. Holt, Membrane processes in energy supply for an osmotic power plant, Desalination 224 (2008) 64–70.
[12] T. Thorsen, T. Holt, The potential for power production from salinity gradients by pressure retarded osmosis, J. Membr. Sci. 335 (2009) 103–110.
[13] N.Y. Yip, A. Tiraferri, W.A. Phillip, J.D. Schiffman, L.A. Hoover, Y.C. Kim, M. Elimelech, Thin-film composite pressure retarded osmosis membranes for sustainable power generation from salinity gradients, Environ. Sci. Technol. 45 (2011) 4360–4369.
[14] S. Chou, R. Wang, L. Shi, Q. She, C. Tang, A.G. Fane, Thin-film composite hollow fiber membranes for pressure retarded osmosis (PRO) process with high power density, J. Membr. Sci. 389 (2012) 25–33.
[15] G. Han, P. Wang, T.S. Chung, Highly robust thin-film composite pressure retarded osmosis (PRO) hollow fiber membranes with high power densities for renewable salinity-gradient energy generation, Environ. Sci. Technol. 47 (2013) 8070–8077.
[16] S. Zhang, T.S. Chung, Minimizing the instant and accumulative effects of salt permeability to sustain ultrahigh osmotic power density, Environ. Sci. Technol. 47 (2013) 10085–10092.
[17] A.P. Straub, N.Y. Yip, M. Elimelech, Raising the bar: Increased hydraulic pressure allows unprecedented high power densities in pressure-retarded osmosis, Environ. Sci. Technol. Lett. 1 (2013) 55–59.
[18] G. Han, S. Zhang, X. Li, T.S. Chung, High performance thin film composite pressure retarded osmosis (PRO) membranes for renewable salinity-gradient energy generation, J. Membr. Sci. 440 (2013) 108–121.
[19] Y.C. Kim, J.H. Lee, S.-J. Park, Novel crossflow membrane cell with asymmetric channels: Design and pressure-retarded osmosis performance test, J. Membr. Sci. 476 (2015) 76–86.
[20] A. Achilli, T.Y. Cath, A.E. Childress, Power generation with pressure retarded osmosis: An experimental and theoretical investigation, J. Membr. Sci. 343 (2009) 42–52.
[21] A. Tiraferri, N.Y. Yip, A.P. Straub, S. Romero-Vargas Castrillon, M. Elimelech, A method for the simultaneous determination of transport and structural parameters of forward osmosis membranes, J. Membr. Sci. 444 (2013) 523–538.
[22] G.M. Geise, H.B. Park, A.C. Sagle, B.D. Freeman, J.E. McGrath, Water permeability and water/salt selectivity tradeoff in polymers for desalination, J. Membr. Sci. 369 (2011) 130–138.
[23] K.L. Lee, R.W. Baker, H.K. Lonsdale, Membranes for power generation by pressure-retarded osmosis, J. Membr. Sci. 8 (1981) 141–171.
[24] J.G. Wijmans, R.W. Baker, The solution-diffusion model: A review, J. Membr. Sci. 107 (1995) 1–21.
[25] A.P. Straub, S. Lin, M. Elimelech, Module-scale analysis of pressure retarded osmosis: Performance limitations and implications for full-scale operation, Environ. Sci. Technol. 48 (2014) 12435–12444.
[26] Q. She, X. Jin, C.Y. Tang, Osmotic power production from salinity gradient resource by pressure retarded osmosis: Effects of operating conditions and reverse solute diffusion, J. Membr. Sci. 401–402 (2012) 262–273.
[27] G. Schock, A. Miquel, Mass transfer and pressure loss in spiral wound modules, Desalination 64 (1987) 339–352.
[28] A.R. Da Costa, A.G. Fane, D.E. Wiley, Spacer characterization and pressure drop modelling in spacer-filled channels for ultrafiltration, J. Membr. Sci. 87 (1994) 79–98.
[29] J. Schwinge, P.R. Neal, D.E. Wiley, D.F. Fletcher, A.G. Fane, Spiral wound modules and spacers: Review and analysis, J. Membr. Sci. 242 (2004) 129–153.
[30] Y.C. Kim, M. Elimelech, Adverse impact of feed channel spacers on the performance of pressure retarded osmosis, Environ. Sci. Technol. 46 (2012) 4673–4681.